ELSEVIER

Journal of Nuclear Materials 241–243 (1997) 505–510

journal of nuclear materials

# Particle balance modelling in ergodic divertor experiments on Tore Supra

T. Loarer *, B. Meslin, Ph. Ghendrih, C. Grisolia, A. Grosman

*Association EURATOM-CEA stir la fusion contrôlée, CEN Cadarache, F-13108 St. Paul-Les-Durance Cédex, France*

**Abstract**

The particle balance and the evaluation of the impact of the plasma edge characteristics in the open divertor configuration (no neutral baffling) is performed with a three reservoir model. The control of the plasma density in the divertor volume is analyzed with respect to the wall behaviour and to the screening capability of the stochastic boundary. The present modelling particularly shows the important role of both the edge electron temperature and the characteristic width of the ergodic layer. Active pumping in conjunction with the establishment of a stochastic boundary is demonstrated to be essential for the precise control of the boundary density, required both to obtain high radiation conditions and good coupling of the auxiliary heating power. This model is compared to a typical ergodic divertor experiment with and without ICRH auxiliary heating and characterised by about 70% of radiated power and achieved with strong $D_2$ gas injections balanced by active pumping. The radiation enhancement by a factor 3.5 from the Ohmic phase to the ICRH phase is achieved with an increase by 15% of the bulk carbon contamination deduced from the increase in $Z_{eff}$. The qualitative agreement between the three reservoir model and the experimental results is presented.

*Keywords:* Tore Supra; Ergodic divertor; Analytic model; Particle balance; Active pumping

## 1. Introduction

In next step devices, a large fraction (> 70%) of the total power will have to be radiated in order to avoid excessive erosion and/or local destruction of the plasma facing components. Highly radiating edge conditions have been demonstrated to be an attractive solution for reducing the power flux density on the limiter [1] or the divertor plate [2]. It is therefore important to achieve particle exhaust to control the plasma density in such conditions.

In order to reduce the convective heat flux on the plasma facing components, the ergodic divertor (ED) may provide a solution for producing a high density, low temperature, highly recycling, highly radiating region at the plasma edge while minimizing bulk contamination [3].

The superconducting tokamak Tore Supra is equipped with six ergodic divertor modules [4] but in the present configuration, the ED neutralizer plates of the six modules cannot handle a total convective heat power larger than 0.7 MW in steady state. However, the enhanced radiation observed in the ED configuration allows plasma operations with total power up to 7 MW. Experiments with attached plasmas have shown that the Tore Supra ED allows an increase of the total radiated power at the edge while minimizing the plasma contamination via edge screening of impurity influxes [5]. Even in the absence of extrinsic impurities, which may provide an even larger radiation fraction, the intrinsic ones (mainly carbon in Tore Supra) associated to the recycling species ($H_2$, $D_2$, He) yield radiation fractions as large as 70%. Experiments with D plasmas leaning on the ED have been performed with active pumping and it has been demonstrated that plasma density control can be obtained while maintaining both the screening of the impurities by the ED and up to 70% of radiation [5–7]. Thus, modelling the plasma density evolu-

* Corresponding author. Tel.: +33-4 42 25 63 32; fax: +33-4 42 25 62 33.


*PII* S0022-3115(96)00554-5

tion as a function of the global recycling conditions (auxiliary heating, attached or detached plasma...) is important for a better understanding of plasma surface interactions as well as for plasma density control and screening of the impurities.

The present paper reports a three reservoir model showing the important role of both the characteristic width $\lambda_s$ of the ergodic boundary layer (or the scrape off layer) and the edge electron temperature for the impurity screening. Analyses of the particle balance for the presented experiment are addressed which shows the role of the ratio between the mean free path of ionisation $\lambda_i$ and $\lambda_s$. Particle balance for different plasma configurations are discussed in which the resulting plasma density is demonstrated to be particularly linked to the wall behaviour. A typical experiment of a D plasma leaning on the energized ED with and without auxiliary heating and with active pumping is presented in the second section. Finally, the different regimes of global recycling of this shot are discussed using the model. The screening efficiency, the pumping as well as the wall behaviour on the particle balance are presented.

## 2. Modelling

### 2.1. Particle reservoir

Modelling of the plasma density evolution with reservoirs (plasma, edge and wall) have been proposed for many configurations [8–10]. In these descriptions one of the main weaknesses is the strong dependence on the characteristic times of the different reservoirs which govern the plasma density responses. Indeed, many solutions can satisfy these models and the characteristic time of each reservoir is difficult to estimate. Finally, the modifications of plasma surface interactions were taken into account by a modification of one of these time constants. Nevertheless, all these models demonstrated the dominant role of the wall particle content in the particle balance. Furthermore, they indicate, through a comparison with experimental results, that a modelling with three reservoirs appears well adapted to describe the plasma density evolution.

The present model is also divided in three reservoirs: the plasma core, an intermediate zone at the edge (SOL or ergodic layer) and the wall. The idea is to take into account the characteristic dimensions $\lambda_s$ and the temperature effect in the intermediate zone, which corresponds in fact to the screening layer [5]. Then, a variation of $\lambda_s$ proportional to the current in the divertor $I_{div}$ modifies the nature of the SOL or of the ergodic layer. In this model, the source, composed of both recycling and external gas flux, provides only particles to the intermediate zone and to the wall. The evolution of the particle content in the plasma ($N_p$)in the intermediate zone ($N_i$) and in the wall ($N_w$) is described by the following system of three coupled equations:

$$\frac{\partial N_p}{\partial t} = -\frac{N_p}{\tau_p} + \frac{N_i}{\tau_{ip}}, \tag{1}$$

$$\frac{\partial N_i}{\partial t} = -\frac{\partial N_p}{\partial_t} + \left(\Phi_0 + \frac{N_w}{\tau_w}\right)\exp\left(\frac{-N_i\langle\sigma\nu\rangle_i}{\nu_0 \mathrm{Vol}_i}\lambda_s\right) - \frac{N_i}{\tau_{iw}}, \tag{2}$$

$$\frac{\partial N_w}{\partial t} = \left(\Phi_0 + \frac{N_w}{\tau_w}\right)\left\{1 - \exp\left(\frac{-N_i\langle\sigma\nu\rangle_i}{\nu_0 \mathrm{Vol}_i}\lambda_s\right)\right\} + \frac{N_i}{\tau_{iw}} - \frac{N_w}{\tau_w}, \tag{3}$$

where $\tau_p$, $\tau_{ip}$, $\tau_{iw}$ and $\tau_w$ are respectively the characteristic residence times of the particles in the plasma, between the intermediate zone and the plasma, between the intermediate zone and the wall and in the wall. $\Phi_0$ is the injected flux, $\langle\sigma\nu\rangle_i$ the ionisation cross section, $\nu_0$ the velocity of the neutrals and $\mathrm{Vol}_i$ is the volume of the intermediate zone.

Noting that $\lambda_i = \nu_0 \mathrm{Vol}_i / N_i\langle\sigma\nu\rangle_i$, the three principal experimental regimes can be described as follows. In a pure divertor regime with an attached plasma ($\lambda_s \gg \lambda_i$), there is a small proportion of particles coming from the injection and from the wall in the intermediate zone (check with Eq. (2)): the injected flux loads the wall principally. For the pure limiter regime ($\lambda_s \approx \lambda_i$), there is about the same proportion of those particles in the intermediate zone and in the wall. In detached plasma conditions ($\lambda_s \ll \lambda_i$), the source feeds particles exclusively in the intermediate zone, the particle balance can be described by 2 reservoirs: the intermediate zone and the plasma. Finally, $N_i$ is proportional to $\langle\sigma\nu\rangle_i$, $N_i T_e^{\gamma}$ is maintained constant with $\gamma < 1$, the averaged edge temperature $T_e$ is initially fixed at 30 eV while the flux delivered by the wall $\Phi_{wall} = N_w/\tau_w$ is assumed to be constant.

The following discussion is devoted to both the time evolution of the plasma content: $N = N_p + N_i$ as well as to the equilibrium which can be obtained for steady state regimes.

Considering an initial equilibrium (I) with the wall for a nil injection, a plasma content $N_0$ is reached. A reference value $N^*$ is fixed for $N$ ($N^*/N_0 = 1.75$ in the chosen example). The gas injection is applied proportionally to the difference ($N^* - N$) point Fig. 1 shows the time evolution of the calculated plasma particle content $N$ normalised to $N_0$ from the equilibrium state $N_0$ up to the reference level $N^*$. It gives also the time evolution of the corresponding injection $\Phi_0/\Phi_{wall}$.

Consequently, Fig. 2 shows the points of the normalised particle content $N/N_0$ as a function of $\Phi_0/\Phi_{wall}$.

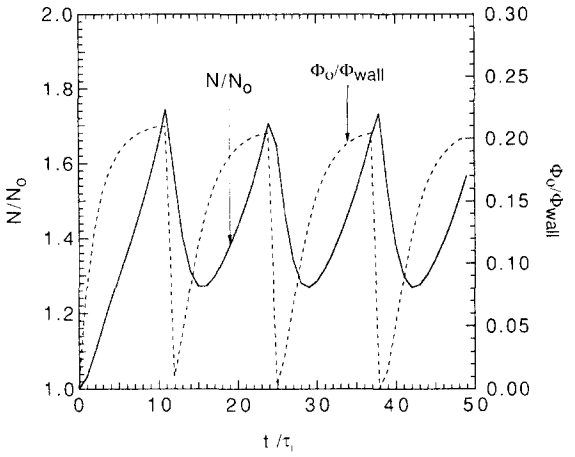


Fig. 1. Evolution of the ratio of both $N/N_0$ and $\Phi_0/\Phi_{wall}$ as a function of the characteristic time of the intermediate zone.

Note that the time evolution of $N/N_0$ would be the same with active pumping, just shifting the initial point of the diagram (0, 1) to the point ($\Phi_{pumped}/\Phi_{wall}$, 1) where $\Phi_{pumped}$ is the pumped flux. In this case, an exhaust efficiency can be defined as the ratio of the particle flux exhausted by the pumping system on the particle flux provided by the wall $\Phi_{pumped}/\Phi_{wall}$.

In the present example, it can be seen that the ratio $\Phi_0/\Phi_{wall}$ must be increased to values larger than 0.15 before getting a significant change in the resulting density, indicating a modest fuelling efficiency at the beginning. When the density becomes larger, the fuelling efficiency increases very rapidly as soon as the edge temperature decreases and the ionisation depth increases. Indeed, $\langle\sigma\nu\rangle_i$ strongly depends on the electron temperature $T_e$ and it can decrease by one order of magnitude when $T_e$ is reduced [11] to values lower than $\approx 15$ eV. When $N$ is close to the reference value, $\Phi_0$ is cut off which leads immediately to the point (0, 1.75). The pumping by the wall reduces the plasma density and consequently $\Phi_0$ is turned on in order to compensate the density drop and so on.

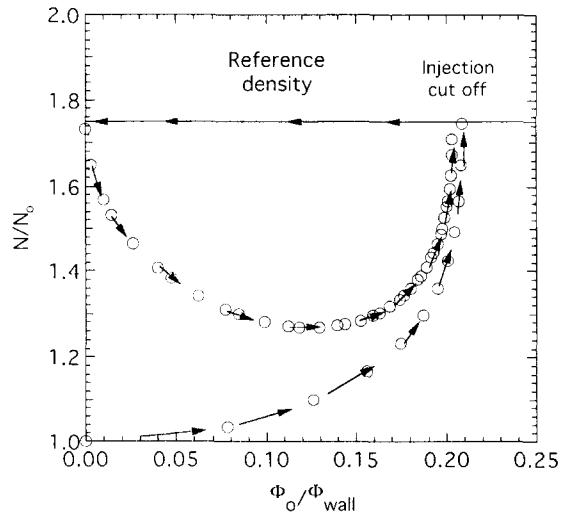


Fig. 2. Evolution of the reference density ratio $N/N_0$ as a function of the ratio $\Phi_0/\Phi_{wall}$. The circles correspond to the time evolution in the cycle for a reference density ratio fixed at 1.75.

### 2.2. Steady state condition

Considering the initial equilibrium state with the wall (I), Eq. (3) becomes

$$\Phi_{wall} = \frac{N_{i0}}{\tau_{iw}} \exp\left( \frac{N_{i0}\langle\sigma\nu\rangle_0}{\nu_0 \mathrm{Vol}_i} \lambda_s \right), \tag{4}$$

where $N_{i0}$ and $\langle\sigma\nu\rangle_0$ are respectively the initial particle content in the intermediate zone and the initial ionisation cross section ($T_e = 30$ eV).

After an injection, a new equilibrium is reached: $\partial N_p/\partial t = \partial N_i/\partial t = 0$. According to Eqs. (2) and (4):

$$\left( \frac{\Phi_0}{\Phi_{wall}} + 1 \right) \frac{N_{i0}}{\tau_{iw}} \exp\left\{ \frac{\lambda_s}{\nu_0 \mathrm{Vol}_i} \left( N_{i0}\langle\sigma\nu\rangle_{i0} - N_{ieq}\langle\sigma\nu\rangle_i \right) \right\} - \frac{N_{ieq}}{\tau_{iw}} = 0, \tag{5}$$

where $N_{ieq}$ is the equilibrium particle number of the intermediate zone.

Moreover, $N_i = (\tau_{ip}/\tau_p)N_p \approx (\tau_{ip}/\tau_p)N$ since the characteristic evolution time in the plasma reservoir is long compared to those of the intermediate zone, Eq. (5) leads to:

$$\frac{\Phi_0}{\Phi_{wall}} = \frac{N_{eq}}{N_0} \exp\left\{ \frac{\tau_{ip}}{\tau_p} \frac{N_0\langle\sigma\nu\rangle_0}{\nu_0 \mathrm{Vol}_i} \lambda_s \left( \frac{\langle\sigma\nu\rangle_i}{\langle\sigma\nu\rangle_0} \frac{N_{eq}}{N_0} - 1 \right) \right\} - 1, \tag{6}$$

where $N_{eq}$ is the total particle number of the plasma at the equilibrium.

Thus, for a defined geometry $\lambda_s$, which depends on the ergodic divertor perturbation, each injection flux determines an equilibrium state. The 'S' shaped curve on Fig. 3 represents the equilibrium states of $N_{eq}/N_0$ locus. For an adiabatic gas injection, the density should follow the stable branches of the curve, but in practice the injection rate is large and there is a departure from this curve (compare Figs. 2 and 3). For a gas injection 'along the curve', the model shows that reaching A the injection cannot be continued without a bifurcation from the equilibrium between the intermediate zone and the wall. At this density limit the plasma is close to detachment. Experimentally like in the model, the edge temperature is very low and the variation of the plasma content can increase abruptly for an injection maintained constant. It is worth noting that

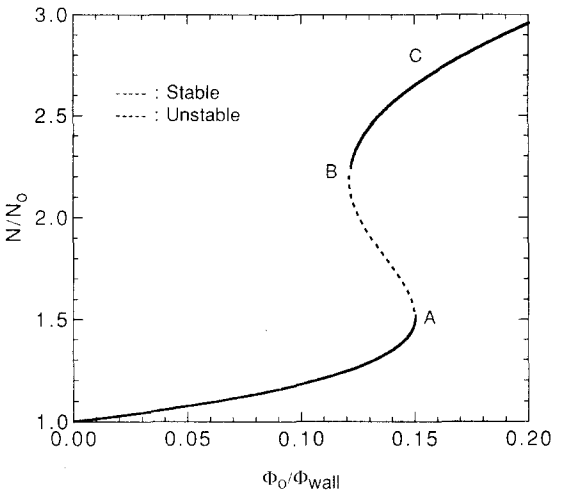


Fig. 3. Density ratio $N/N_0$ as a function of $\Phi_0/\Phi_{wall}$ for steady state.

due to the screening by the ergodic layer, the transition towards detachment occurs at a lower value of the ratio $\Phi_0/\Phi_{wall}$.

Detached plasmas are difficult to stabilise and they can cause disruptions. Some of the equilibrium states of $N_{eq}/N_0$ are unstable: for $dN_{eq}/d\Phi_0 < 0$ (between A and B in Fig. 3). If the feedback reference point is set in the unstable zone (A–B), $N_i$ cannot reach the equilibrium so that a relaxation via gas injection cut off will occur. The branch (C) in Fig. 3 can be considered as an unstable equilibrium for reasons which are extrinsic to the model (MHD).

This model describes rather well the experimental density build up, which also strongly depends on the wall conditioning [12]. Indeed, as the impurity content of the discharge increases, the edge temperature decreases and the bifurcation at the point A shifts to both lower critical gas injection and lower plasma density.

## 3. Comparison with experimental results

### 3.1. Experiment

The reported experiment describes a typical D shot with auxiliary heating and active pumping where the plasma is limited on the ED modules; the time evolution of the main parameters of this shot are displayed on Fig. 4. The plasma current is $I_p = 1.5$ MA and the toroidal field is $B_T = 3.4$ T to satisfy the resonance condition at the edge ($q_{edge} \approx 3$); the ED is switched on during the plasma current ramp-up $t \approx 1$ s and energized at its maximum current ($I_{div} = 45$ kA). Fig. 4a shows the time behaviour of $I_p$, $I_{div}$ and of the volume averaged plasma density $\langle n_e \rangle$. Fig. 4b displays the gas injection (which is feedback controlled to obtain $\langle n_e \rangle \approx 3.2 \times 10^{19}$ m$^{-3}$) and the pumped flux. Two ICRH pulses are applied from 4.5 to 6 s and from 7 to 8.5 s respectively, at a power level of 3.8 MW and at 2 MW (Fig. 4c). Finally, Fig. 4d displays the resulting radiated power as a function of time as well as the $Z_{eff}$ deduced from Bremsstrahlung measurements.

It should be noted that in spite of the increase of the plasma density as soon as the additional power is applied, the plasma density level reaches a quasi steady state during each of the two additional heating periods. Moreover a high gas injection rate is required to maintain the density constant, demonstrating the effect of the active pumping [7]. During the first ICRH pulse, the plasma density is constant until an increase of a copper line emission from the bulk appears. The radiation instantaneously increases while the plasma coupling resistance drops immediately,

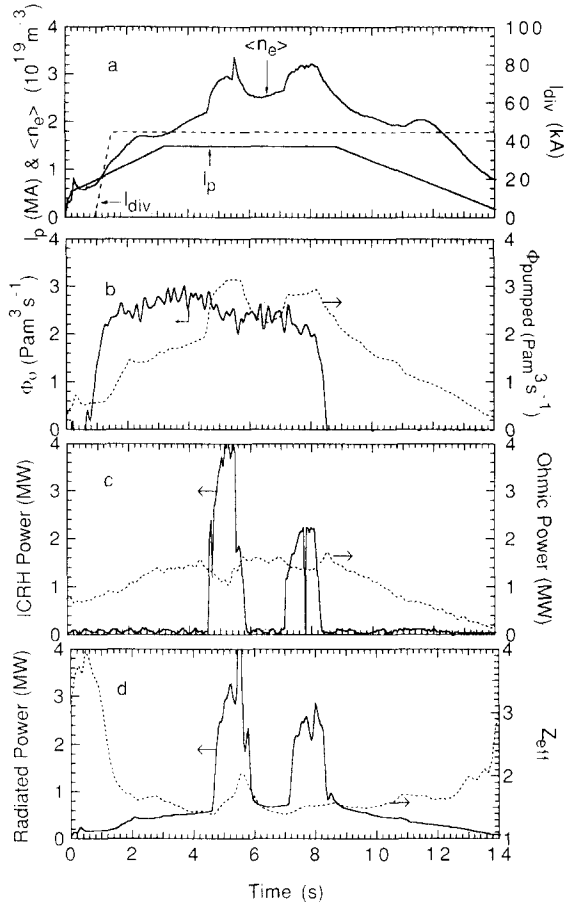


Fig. 4. General plasma characteristics of a D shot leaning on the ED with additional power and active pumping. (a) Plasma current $I_p$, plasma density $\langle n_e \rangle$ and current in the ergodic divertor $I_{div}$ as a function of time. (b) Time evolutions of gas injection $\Phi_0$ and pumped flux $\Phi_{pumped}$. (c) ICRH and Ohmic power as a function of time. (d) Radiated power $P_{rad}$ and resulting $Z_{eff}$ of the plasma as a function of time.

causing a cutoff of the power. During this pulse, about 60% of the total power (5.0 MW, of which 1.2 MW Ohmic and 3.8 MW ICRH) is radiated in spite of the medium plasma density $\langle n_e \rangle \approx 3 \times 10^{19}$ m$^{-3}$. The $Z_{eff}$ has a sharp increase in correspondence of the copper influx, which is probably coming from actively cooled copper elements in the ICRH antenna.

During the second pulse, the higher plasma density corresponds to a higher radiation fraction which increases to 70% (of which 80–90% from the ergodic layer and respectively 20–10% from the bulk) in steady state (Fig. 4d). It can also be seen that there is no significant impurity generation, as demonstrated by the $Z_{eff}$ which only increases by about 15%. When the input power increases, the electron temperature at the edge increases, but the ergodic layer still allows the preservation of the impurity screening efficiency already observed with the ED for the Ohmic phase [5]. A steady state plasma density is obtained with a strong gas injection compensated by active pumping. Finally, when both the ICRH and the gas injection are cut off, the plasma density decays very rapidly, with a characteristic time of $\tau_p^*$ of $\approx 1$ s, resulting from strong active pumping as well as from changes of the recycling at the edge when the ICRH power is stopped ($\tau_p$ depends on the total power input of the plasma [14]). The particle exhaust efficiency can be determined between the two ICRH pulses; in these conditions, the plasma density is constant and the strong gas injection of 2.5 Pa m$^3$ s$^{-1}$ is balanced by the active pumping. The resulting Ohmic exhaust efficiency $\varepsilon$ is estimated to be 25% for the Ohmic phase (assuming $\tau_p = 0.5$ s [6]) while for the ICRH phases, the abrupt increase of the plasma density at the beginning of the pulse leads to a reduction of the gas injection and consequently to a reduction of $\varepsilon$, which is estimated to be about 20% ($\tau_p \approx 0.3$ s with 3 MW of total power [14]).

For the shot described above it can be seen that there are different regimes of global recycling with and without auxiliary heating which are now discussed using the model.

### 3.2. Interpretation of the experiment with the model

This model particularly shows the important role of $\lambda_s$ on the resulting plasma density. When the ED is energized and when the resonance condition at the edge is satisfied, the mean free path of ionisation of D neutrals in the ergodic layer is significantly lower than $\lambda_s$.

Therefore, in spite of the rather medium plasma density which allows for larger fuelling efficiency, a strong gas injection is always required to increase the density with the ED compared to the limiter case. Experimentally this phenomenon is observed in the plasma and density ramp up (Fig. 4a, b, $t = 0$–3 s) where it can be seen that the density increases rapidly in limiter configuration while it is strongly reduced as soon as the resonance condition with the ED is obtained ($t \approx 3$ s) and in spite of a roughly constant gas injection. Moreover, in the present example, the active pumping by the ED strengthens the screening efficiency.

The interpretation, in terms of $\lambda_s$ and $T_e$, of the effects of the auxiliary heating on the density is more difficult. Indeed, when the auxiliary heating is applied, the particle flux from the wall increases but, as already noticed, the wall is not changed in the present version of the model. However, the experimental increase $\Phi_{wall}$ can be described by an abrupt increase of the source $\Phi_0$ in the model. Therefore, as soon as the auxiliary heating is applied, on Fig. 3, a new equilibrium is reached immediately by shifting the equilibrium point to both a larger gas injection and plasma density. Also, it is worth noting that when applying auxiliary heating the fraction of backscattered atoms increases ($\nu_0$) with $T_e$ and this can be interpreted as a reduction of $\lambda_s$. Finally, as observed on the IR views of the neutraliser plates, just at the beginning of the ICRH pulse, the plasma locally detaches [13]; in these conditions, the neutrals can penetrate into the plasma [7]. In practice, it is believed that both the reduction in $\lambda_s$ and the increase neutral fuelling efficiency at detachment lead to the abrupt increase of the plasma density. The opposite phenomena is observed when the power is cut off; the plasma density drop is always very strong, suggesting a sudden increase of $\lambda_s$ which can give an idea of the screening efficiency of the intermediate layer.

This model also allows one to describe the plasma density evolution with and without the ED energized since $\lambda_s$ is proportional to $I_{div}$. Indeed, the screening efficiency of the ED is demonstrated to be larger than those of the limiter configuration; such a comparison can be interpreted as a reduction of $\lambda_s$ when turning off the ED as well as a larger temperature at the edge. In these conditions the plasma density increases immediately since the mean free path of ionisation $\lambda_i$ of the neutral becomes close to those of the SOL while in the ED configuration $\lambda_i$ is significantly smaller than the ergodic layer characteristic thickness [5]. Experimentally, this effect is illustrated on Fig. 4b at the transition of the ED to limiter configuration ($t \approx 11.2$ s) during the ramp down of the plasma current when the resonance condition is lost.

Finally, during the first ICRH pulse, the copper emission leads to an enhance radiation at the edge. The resulting cooling effect on $T_e$ is a strong reduction of $\langle \sigma v \rangle_i$ in the ergodic boundary layer and consequently the copper penetrates the discharge as monitored by the visible spectroscopy signal and $Z_{eff}$.

## 4. Summary and conclusion

The present modelling of the global particle balance allows one to describe the resulting plasma density which is shown to be particularly linked to both the wall behaviour and the screening capability of the ergodic boundary layer. The role of the ratio $\lambda_i/\lambda_s$ is demonstrated to be

dominant for the screening of the deuterium as well as of the impurity by the intermediate zone. This model also reports quite well the transition from attached to detached plasma showing the importance of the active pumping in order to control this transition. A qualitative agreement of the results of this model with experimental observations is obtained for the different global recycling conditions of a typical ED shot with active pumping and with and without auxiliary heating. Finally, in order to improve this model, the next step will have to include a possible variation of the wall flux as well as to provide quantitative comparison with experimental data.

## Acknowledgements

The authors would like to acknowledge the permanent technical support provided by J.Y. Pascal and S.J. Vartanian.

## References

[1] U. Samm, G. Bertschinger, P. Bogen et al., Plasma Phys. Controlled Fusion 35(12) (1993) B167.
[2] G.C. Vlases, Plasma Phys. Controlled Fusion 35(12) (1993) B67.
[3] A. Samain, A. Grosman and W. Feneberg, J. Nucl. Mater. 111–112 (1982) 408.
[4] A. Grosman, T.E. Evans, Ph. Ghendrih et al., J. Nucl. Mater. 176–177 (1990) 493.
[5] Ph. Ghendrih, A. Grosman and H. Capes, Report EUR-CEA-FC-1571, Plasma Phys. Controlled Fusion 38 91996) 1653–1724.
[6] T. Loarer, M. Chatelier, A. Grosman et al., Plasma Phys. Controlled Fusion 37(11) (1995) A203–A214.
[7] T. Loarer, M. Chatelier, A. Grosman et al., J. Nucl. Mater. 220–222 (1995) 183.
[8] C. Grisolia, Ph. Ghendrih, B. Pégourié et al. J. Nucl. Mater. 196–198 (1992) 281.
[9] L.D. Horton, P. Andrew, G. Bracco et al., J. Nucl. Mater. 196–198 (1992) 139.
[10] E. Tsitrone, C. Grisolia, Ph. Ghendrih et al., CEN Cadarache, Tore Supra, July 1993, private communication.
[11] P.C. Stangeby and G.M. McCracken, Nucl. Fusion 30(7) (1990) 1225.
[12] C. Grisolia, C. Chamouard, Ph. Ghendrih et al., 22nd EPS Conf., Bournemouth, Vol. 19C, part IV (1995).
[13] A. Grosman et al., these Proceedings, p. 532.
[14] B. Pégourié et al., these Proceedings, p. 494.